# Ultra-compact photonic crystal waveguide spatial mode converter and its connection to the optical diode effect

**Victor Liu,* David A. B. Miller, and Shanhui Fan**

*Department of Electrical Engineering, Stanford University, Stanford, California 94305 USA*

*vkl@stanford.edu

**Abstract:** We design an extremely compact photonic crystal waveguide spatial mode converter which converts the fundamental even mode to the higher order odd mode with nearly 100% efficiency. We adapt a previously developed design and optimization process that allows these types of devices to be designed in a matter of minutes. We also present an extremely compact optical diode device and clarify its general properties and its relation to spatial mode converters. Finally, we connect the results here to a general theory on the complexity of optical designs.



**OCIS codes:** (130.3120) Integrated optics devices; (130.2790) Guided waves; (230.3120) Integrated optics devices.

## References and links

1. J. Wang, J.-Y. Yang, I. M. Fazal, N. Ahmed, Y. Yan, H. Huang, Y. Ren, Y. Yue, S. Dolinar, M. Tur, and A. E. Willner, "Terabit free-space data transmission employing orbital angular momentum multiplexing," Nat. Photon. **6**, 488–496 (2012).
2. L. H. Gabrielli, D. Liu, S. G. Johnson, and M. Lipson, "On-chip transformation optics for multimode waveguide bends," Nat. Commun. **3**, 1217 (2012).
3. D. A. B. Miller, "All linear optical devices are mode converters," Opt. Express **20**, 23985–23993 (2012).
4. D. A. B. Miller, "How complicated must an optical component be?," Submitted to J. Opt. Soc. Am. A. http://arxiv.org/abs/1209.5499.
5. V. P. Tzolov and M. Fontaine, "A passive polarization converter free of longitudinally-periodic structure," Opt. Commun. **127**, 7–13 (1996).
6. T. D. Happ, M. Kamp, and A. Forchel, "Photonic crystal tapers for ultracompact mode conversion," Opt. Lett. **26**, 1102–1104 (2001).
7. A. Talneau, P. Lalanne, M. Agio, and C. M. Soukoulis, "Low-reflection photonic-crystal taper for efficient coupling between guide sections of arbitrary widths," Opt. Lett. **27**, 1522–1524 (2002).
8. P. Sanchis, J. Marti, A. Garcia, A. Martinez, and J. Blasco, "High efficiency coupling technique for planar photonic crystal waveguides," Electron. Lett. **38**, 961–962 (2002).
9. P. Lalanne and A. Talneau, "Modal conversion with artificial materials for photonic-crystal waveguides," Opt. Express **10**, 354–359 (2002).
10. P. Bienstman, S. Assefa, S. G. Johnson, J. D. Joannopoulos, G. S. Petrich, and L. A. Kolodziejski, "Taper structures for coupling into photonic crystal slab waveguides," J. Opt. Soc. Am. B **20**, 1817–1821 (2003).
11. E. Khoo, A. Liu, and J. Wu, "Nonuniform photonic crystal taper for high-efficiency mode coupling," Opt. Express **13**, 7748–7759 (2005).
12. J. Castro, D. F. Geraghty, S. Honkanen, C. M. Greiner, D. Iazikov, and T. W. Mossberg, "Demonstration of mode conversion using anti-symmetric waveguide bragg gratings," Opt. Express **13**, 4180–4184 (2005).
13. S. Y. Tseng and M. C. Wu, "Adiabatic mode conversion in multimode waveguides using computer-generated planar holograms," IEEE Photon. Technol. Lett. **22**, 1211–1213 (2010).
14. P. Sanchis, J. Marti, J. Blasco, A. Martinez, and A. Garcia, "Mode matching technique for highly efficient coupling between dielectric waveguides and planar photonic crystal circuits," Opt. Express **10**, 1391–1397 (2002).
15. I. L. Gheorma, S. Haas, and A. F. J. Levi, "Aperiodic nanophotonic design," J. Appl. Phys. **95**, 1420–1426 (2004).

#178467 - $15.00 USD Received 22 Oct 2012; revised 19 Nov 2012; accepted 23 Nov 2012; published 6 Dec 2012

16. Y. Jiao, S. Fan, and D. A. B. Miller, "Demonstration of systematic photonic crystal device design and optimization by low-rank adjustments: an extremely compact mode separator," Opt. Lett. **30**, 141–143 (2005).
17. V. Liu, Y. Jiao, D. A. B. Miller, and S. Fan, "Design methodology for compact photonic-crystal-based wavelength division multiplexers," Opt. Lett. **36**, 591–593 (2011).
18. G. G. Denisov, G. I. Kalynova, and D. I. Sobolev, "Method for synthesis of waveguide mode converters," Radiophys. Quantum El. **47**, 615–620 (2004).
19. M. Qiu, "Effective index method for heterostructure-slab-waveguide-based two-dimensional photonic crystals," Appl. Phys. Lett. **81**, 1163–1165 (2002).
20. Y. Li and J.-M. Jin, "A vector dual-primal finite element tearing and interconnecting method for solving 3-D large-scale electromagnetic problems," IEEE Trans. Antennas Propag. **54**, 3000–3009 (2006).
21. G. Veronis, R. W. Dutton, and S. Fan, "Method for sensitivity analysis of photonic crystal devices," Opt. Lett. **29**, 2288–2290 (2004).
22. Y. Jiao, S. Fan, and D. A. B. Miller, "Systematic photonic crystal device design: global and local optimization and sensitivity analysis," IEEE J. Quantum Elect. **42**, 266–279 (2006).
23. V. Liu, D. A. B. Miller, and S. Fan, "Highly tailored computational electromagnetics methods for nanophotonic design and discovery," Proc. IEEE (Accepted).
24. Y. Huang and Y. Y. Lu, "Scattering from periodic arrays of cylinders by dirichlet-to-neumann maps," J. Lightwave Technol. **24**, 3448–3453 (2006).
25. Z. Hu and Y. Y. Lu, "Efficient analysis of photonic crystal devices by dirichlet-to-neumann maps," Opt. Express **16**, 17383–17399 (2008).
26. M. Greenberg and M. Orenstein, "Irreversible coupling by use of dissipative optics," Opt. Lett. **29**, 451–453 (2004).
27. L. Feng, M. Ayache, J. Huang, Y.-L. Xu, M.-H. Lu, Y.-F. Chen, Y. Fainman, and A. Scherer, "Nonreciprocal light propagation in a silicon photonic circuit," Science **333**, 729–733 (2011).
28. A. E. Serebryannikov, "One-way diffraction effects in photonic crystal gratings made of isotropic materials," Phys. Rev. B **80**, 155117 (2009).
29. C. Wang, C.-Z. Zhou, and Z.-Y. Li, "On-chip optical diode based on silicon photonic crystal heterojunctions," Opt. Express **19**, 26948–26955 (2011).
30. C. Lu, X. Hu, H. Yang, and Q. Gong, "Ultrahigh-contrast and wideband nanoscale photonic crystal all-optical diode," Opt. Lett. **36**, 4668–4670 (2011).
31. S. Fan, R. Baets, A. Petrov, Z. Yu, J. D. Joannopoulos, W. Freude, A. Melloni, M. Popović, M. Vanwolleghem, D. Jalas, M. Eich, M. Krause, H. Renner, E. Brinkmeyer, and C. R. Doerr, Comment on "nonreciprocal light propagation in a silicon photonic circuit," Science **335**, 38 (2012).

## 1. Introduction

There is growing interest using multiple spatial modes in optical systems to increase information processing capacity [1]. Much of the existing work has been focused on fiber optic communications, but there is also interest in developing integrated on-chip applications [2]. The basic building blocks of these systems are components that can perform spatial mode manipulation with minimal crosstalk over a wide bandwidth. Also, from a more fundamental point of view, spatial mode manipulation has provided a model to understand complexities in optical devices in general [3, 4].

One important class of devices is those that convert one waveguide mode into another. Aside from applications which require their explicit functionality, mode converters are necessary to excite higher order waveguide modes due to the difficulty in coupling modes other than the fundamental into a waveguide from free space. This conversion is conventionally performed adiabatically using tapered waveguide designs that are tens or hundreds of wavelengths long [5–13]. More compact designs have also been shown with good, though still limited, conversion efficiency [14].

We present here an extremely compact photonic crystal waveguide mode converter which converts the fundamental even-symmetric waveguide mode into the second order odd-symmetric mode, and vice versa, in a length of four wavelengths, with nearly 100% conversion efficiency. We also show a smaller structure which performs mode conversion of only one mode and we discuss its relationship to the optical diode effect.

We employ an aperiodic design methodology [15–17] that does not assume the adiabatic

#178467 - $15.00 USD Received 22 Oct 2012; revised 19 Nov 2012; accepted 23 Nov 2012; published 6 Dec 2012

coupling that is typical of existing design approaches [18]. The ability to efficiently design non-trivial compact devices for mode manipulation enables the design of integrated photonic systems which make use of higher order waveguide modes. Although the presented designs are idealized 2D structures, there have been recent efforts to implement such designs using effective index models in 3D for planar fabrication [19]. Full field numerical simulations also verify the functionality of 3D structures based on planar 2D designs [20].

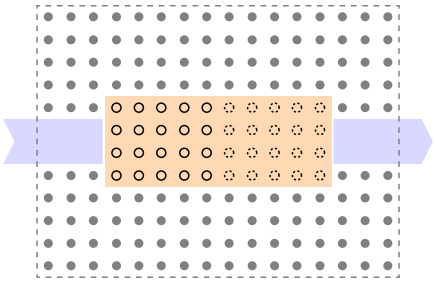

Fig. 1. Schematic of template structure. Background dielectric rods are indicated with solid circles. Black open circles are the 20 rods that can be added or removed, while the black dashed circles are determined automatically by inversion symmetry. The blue highlighted regions show the waveguides, and the orange highlighted region shows the coupler region where search and optimization are performed.

## 2. Mode converter

### *2.1. Design considerations based on general properties of the scattering matrix*

The structures we consider are modifications of a background photonic crystal of silicon rods ($\varepsilon = 12$) of radius $0.2a$ in air ($\varepsilon = 1$) on a square lattice of lattice constant $a$ (Fig. 1). The fields are polarized with the electric field out-of-plane. The input and output waveguides (blue regions in Fig. 1) are formed by removing two lines of rods. These waveguides support two modes: a fundamental even-symmetric mode and a higher order odd-symmetric mode. Our aim is to design the coupler region (orange region in Fig. 1) between the waveguides that enables modal conversion.

An ideal mode-converter device completely converts the fundamental even mode to the higher order odd mode, and completely converts the odd mode to the even mode, as illustrated symbolically with its corresponding scattering matrix in Fig. 2. We will denote by the letters A and B the even and odd modes, respectively, to the left of the coupler. Similarly, the letters C and D will denote the even and odd modes, respectively, to the right of the coupler. The scattering matrix relates the amplitudes of the out-going A, B, C, and D modes (indicated in blue in Fig. 2) to the amplitudes of the in-going A, B, C, and D modes (indicated in red in Fig. 2). Note that the phases of the modes can always be defined to make the scattering matrix have the given form with purely real entries.

Any reciprocal structure that enables 100% transmission of an incident even mode on the left to the odd mode on the right must necessarily provide complete transmission as well for an incident odd mode on the right to the even mode on the left. Such reciprocity holds for any passive and linear structure consisting only of materials described by scalar permittivity and permeability, as is the case here. Analogously, complete transmission of an incident odd mode on the left to the even mode on the right necessarily implies complete transmission of an even mode from the right to the odd mode on the left. Since an ideal mode converter performs both of these conversions, it must have identical behavior in both directions.

#178467 - $15.00 USD Received 22 Oct 2012; revised 19 Nov 2012; accepted 23 Nov 2012; published 6 Dec 2012

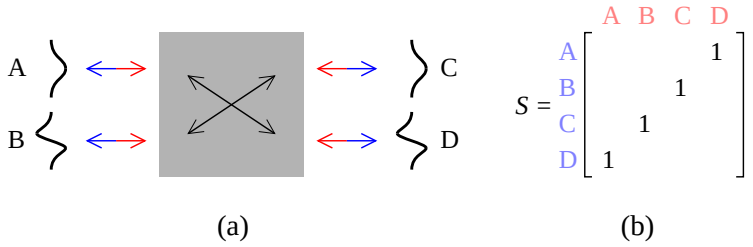


Fig. 2. (a) Ideal mode converter specification. The letters denote different modes. The red and blue arrows represent input and output in each mode, respectively. The gray region represents the converter device. (b) The scattering matrix of the device.

For an ideal mode converter, there is therefore a symmetry in the S-matrix between the left-to-right conversion, and the right-to-left conversion. (This specific desired symmetry for such an ideal mode-converter device is in addition to, and consistent with, the general property that the S-matrix itself must be symmetric for any reciprocal system, as discussed above.) The most direct way to enforce this property of the system is to impose inversion symmetry on the structure. Therefore in the coupler region highlighted in Fig. 1, only the rods on the left represented by solid open circles are design parameters, while the dashed open circles are determined by inversion symmetry.

### *2.2. Numerical design and optimization*

In order to optimize for conversion efficiency as well as bandwidth, the following error metric is used to evaluate designs:

$$J = \sum_{\omega} (1 - p_{\omega})^2 \tag{1}$$

where $p_\omega$ is the conversion efficiency at frequency $\omega$. For the examples shown in the remainder of this paper, we evaluate $J$ by summing the conversion efficiency at a center frequency of $0.4025 \times 2\pi c/a$ and two neighboring frequencies 0.3% above and below.

The design process proceeds in two phases. In the first phase, a combinatorial search is performed where every possible combination of rods (presence or absence) on the 20 lattice sites in the coupler region is considered. In this phase, the rods considered are identical to those in the background photonic crystal (with radius $0.2a$). Any structures encountered in the combinatorial search that show promising conversion behavior ($J \lesssim 0.5$) are considered initial candidates for further optimization.

In the second phase, the initial candidates are fine tuned by adjusting the rod radii in the coupler region using a simple gradient descent method to minimize the error metric $J$ in Eq. (1). The gradient of $J$ with respect to rod radius is straightforward to calculate by applying the adjoint variable method throughout the computational process [21, 22]. In both phases of optimization, in order to limit the design space, we consider only structures with rods centered on the 20 possible lattice sites within the coupler region.

There are a total of $2^{20}$ possible rod configurations, and a systematic enumeration of the entire space of about one million combinations is performed using an efficient simulation method tailored to the particular class of structures being analyzed [23]. The Dirichlet-to-Neumann (DtN) map is used to model each unique type of unit cell [24]. The details of the method have been described thoroughly in [25], but we briefly state the essential details. The DtN map at a single frequency relates the tangential electric field on the boundary of a unit cell to the tangential magnetic field on the boundary. By enforcing field continuity conditions, one then

#178467 - $15.00 USD Received 22 Oct 2012; revised 19 Nov 2012; accepted 23 Nov 2012; published 6 Dec 2012

obtains a linear system $Ax = b$ where $x$ represents the fields on the boundaries of the unit cells, $b$ represents the incident wave source, and $A$ is the system matrix formed from the DtN maps.

In the initial combinatorial search, only two unit cell types are present, so only two different DtN maps need to be computed. For the special case of rods in air, the DtN map can be computed with cylindrical wave expansions, and this basis is sufficiently accurate that only 5 unknowns per unit cell edge are required (verification with 7 unknowns per edge yields essentially identical results). Therefore, for the structures shown, the resulting linear system has dimensions $865^2$. On a local cluster with 80 cores, the entire combinatorial search of $2^{20}$ structures at a single frequency can be completed in 10 minutes, while the subsequent gradient optimization usually takes no longer than 5 minutes on a personal computer.

### *2.3. Results*

One configuration which achieved very high conversion efficiency is shown in Fig. 3. All the rods in this structure are identical ($r = 0.2a$), and further optimization of rod radius did not produce substantial improvement in device performance. As shown in Fig. 3(a), the mode converter exhibits greater than 99% peak conversion efficiency from mode A to mode D with a relative frequency width of 0.176% at the 90% threshold. For a center wavelength at 1.55 $\mu$m, this corresponds to a bandwidth of 2.73 nm. Note that the spectrum for the other three conversion processes (B to C, C to B, D to A) must all have the same spectrum, as required by inversion symmetry and reciprocity. Therefore when considering the scattering matrix of this device, one can immediately see that it performs as a nearly perfect mode converter. Quantitatively, the reflection (from a mode back into the same mode) and crosstalk (conversion efficiency to an unwanted mode) parameters at the operating frequency of $\omega = 0.4025 \times 2\pi c/a$ are all lower than $-45$ dB, demonstrating excellent suppression of undesired behavior. Representative field patterns for the device for the A to D conversion and the B to C conversion are shown in Fig. 3(b). The entire coupler region occupies an area of $4 \times 10$ unit cells, which is about four wavelengths long and two wavelengths wide. To the best of our knowledge, this is the most compact design of a dielectric mode converter at the present time.

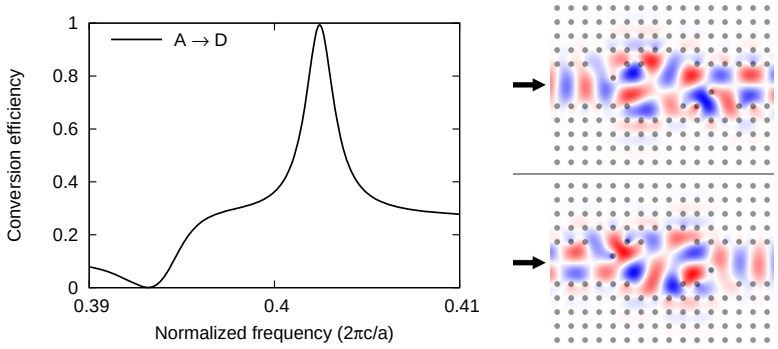


Fig. 3. (a) Spectral conversion efficiency of the mode converter shown in the right side of Fig. 1. (b) Representative field patterns for both input modes from the left at normalized frequency $0.4025 \times 2\pi c/a$.

#178467 - $15.00 USD Received 22 Oct 2012; revised 19 Nov 2012; accepted 23 Nov 2012; published 6 Dec 2012

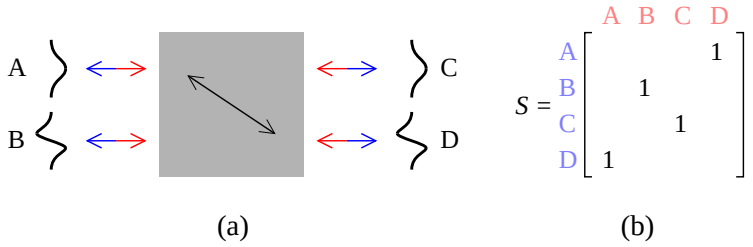


Fig. 4. (a) Ideal optical diode specification. Similar to the ideal mode converter, an input even mode from the left is converted to an odd mode on the right, and vice versa. However, an odd mode from the left or an even mode from the right are completely reflected. (b) The scattering matrix of the device.

## 3. Optical diode

An optical diode is a device similar to the mode converter above, except that it only completely converts a single mode while completely reflecting all other modes. The functionality of an optical diode and its corresponding scattering matrix is summarized in Fig. 4. The even mode A from the left is converted into the odd mode D on the right, while the odd mode B from the left is completely reflected back to the same odd mode B at the left. From the right, the even mode C is completely reflected back to the even mode at the right, while the odd mode D from the right is completely converted to the even mode A to the left. Note the apparent asymmetry in the device behavior when the same mode is sent in from either side of the device (e.g., the even mode is completely transmitted in one direction, but completely reflected in the other direction), hence the word "diode".

There have been numerous reports of such optical diodes [26–30]. Additionally, in the laboratory it is common to use the combination of a polarization beamsplitter and a quarter wave plate to separate forward and reflected backward beams spatially; such a device is an optical diode in the current sense, operating on the two orthogonal input polarizations rather than orthogonal spatial modes. It is important to emphasize that such optical diodes are fully reciprocal devices and cannot perform optical isolation [31], however they do provide an interesting capability for mode manipulation and thus might have potential applications. Previously reported designs of optical diodes operating on spatial (rather than polarization) modes have all been periodic devices which require many periods to achieve efficient mode conversion. Some of these designs, in addition, use materials that have intrinsic loss. In contrast, we present a design which is both compact and uses completely lossless materials.

Since by the very definition of an optical diode there is no symmetry between the left-to-right and the right-to-left conversion processes, the structure cannot have inversion symmetry. We therefore take a smaller coupler optimization region shown in Fig. 5(a) and apply the same optimization strategy as was described in the previous section. The rod configuration shown in Fig. 5(a) corresponds to one particular structure with high conversion efficiency found in the combinatorial search. Further optimization of the radii of the 10 rods in the coupler region yielded the optimized structure shown in Fig. 5(b). A comparison of the conversion efficiency spectrum before and after the rod radius optimization is shown in Fig. 6, showing a clear improvement in both peak conversion efficiency as well as a doubling of the usable bandwidth. The peak conversion efficiencies (mode A to D and mode C to C) at the design frequency $\omega = 0.4025 \times 2\pi c/a$ exceed 97%, while the reflection and crosstalk parameters (the remaining mode conversions) are below $-35$ dB.

Representative field profiles of the optimized structure in operation at the design frequency

#178467 - $15.00 USD Received 22 Oct 2012; revised 19 Nov 2012; accepted 23 Nov 2012; published 6 Dec 2012

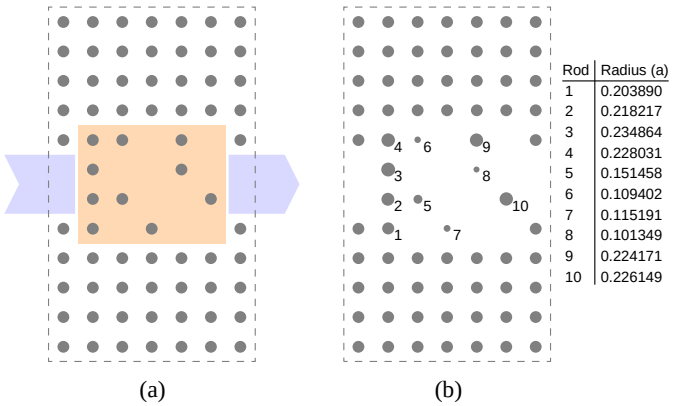


Fig. 5. Schematic of optimized structures. (a) Candidate structure resulting from the combinatorial search. The blue highlighted regions show the waveguides, and the orange highlighted region shows the coupler region where search and optimization are performed. (b) Final rod radius optimized structure of the corresponding structure on the left.

are shown in Fig. 7. The top row shows excitation from the left waveguide, while the bottom row shows excitation from the right waveguide. The field profiles explicitly show the asymmetry of the conversion process for a particular mode. The fundamental mode is completely transmitted from left to right (Fig. 7(a)), while it is completely reflected when incident from the right (Fig. 7(c)). Despite the apparent asymmetry in the conversion properties of this device, this system is completely reciprocal since there is no magneto-optic material or any breaking of time-reversal symmetry. Thus, the scattering matrix of the system is symmetric, as can be seen by comparing Fig. 7(a) and Fig. 7(d).

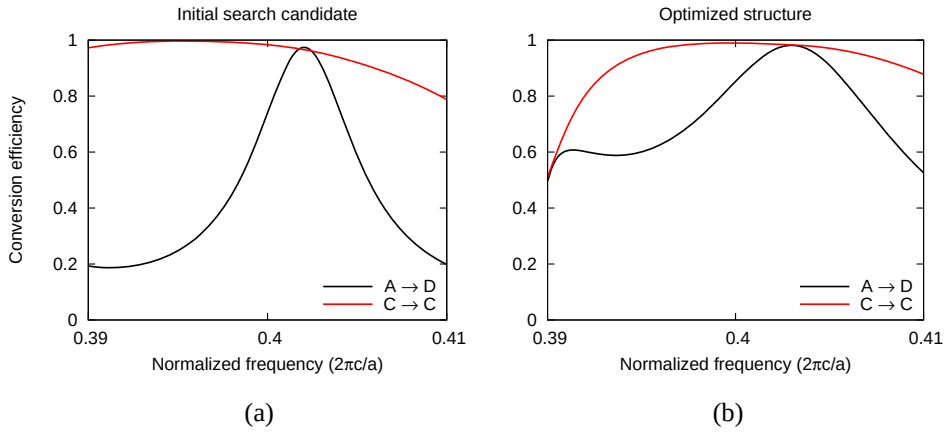


Fig. 6. Spectral conversion efficiency of optical diode device. (a) The transmission spectrum from mode A to mode D (black line) and the reflection spectrum for mode C to mode C (red line) for the unoptimized structure shown in Fig. 5(a). (b) The same spectra for the optimized structure in Fig. 5(b).

Compared with the existing spatial mode diode designs, our design here utilizes only transparent materials that have no intrinsic material loss. It is in a waveguide setting that is directly compatible with integrated photonics. It has probably the smallest design footprint that has

#178467 - $15.00 USD Received 22 Oct 2012; revised 19 Nov 2012; accepted 23 Nov 2012; published 6 Dec 2012

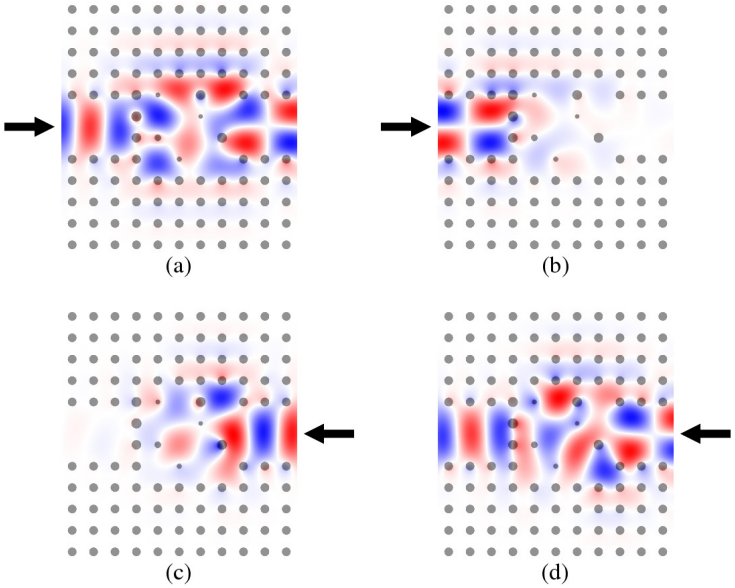


Fig. 7. Field patterns of the radius-optimized optical diode device shown in Fig. 5(b). The top row shows excitation from the left, while the bottom row shows excitation from the right.

ever been reported, and has near ideal performance as far as the apparent contrast in the two directions is concerned.

It is important to emphasize that the structures presented above are not isolated instances of structures exhibiting high conversion efficiency. For example, in the combinatorial search for the optical diode, more than 10 such structures were found, with spectra shown in Fig. 8. Therefore, our design method, when given a sufficiently large search space, is capable of producing many possible designs which might be required if additional design constraints are imposed.

## 4. Design complexity

The numerical design here is directly connected to a general theory on the design complexity of optical devices. We can consider the complexity required in our designs by using the approach of Ref. [4]. In general, it is not possible to state the complexity required for any one device design [4]; we can, however, state the complexity required to choose any one of a family of devices [4]. In the terminology of [4], at least at one specific frequency, the devices in Figs. 1, 2, 4, and 5 have potentially 4 input modes ($M_I = 4$) and 4 output modes ($M_O = 4$). The most general linear device relating input to output modes could therefore be represented by a $4 \times 4$ device matrix, which in this case is the same matrix as the most general $4 \times 4$ scattering matrix. That most general device matrix would require therefore 16 complex numbers, corresponding to 32 real numbers (a "complexity number" $N_D = 32$ [4]) that might have to be specified somewhere in the device design. The devices we design here are presumed to be lossless (and hence represented by a unitary matrix) and reciprocal, and we likely do not care about the phase of the output beams relative to the input beams. We can follow the counting approaches in [4] to establish the complexity number required for an arbitrary device that also satisfies these various constraints and flexibilities. If we wanted to have the freedom to design specific responses for more than one frequency, then in the worst case we would have to multiply the number of

#178467 - $15.00 USD Received 22 Oct 2012; revised 19 Nov 2012; accepted 23 Nov 2012; published 6 Dec 2012

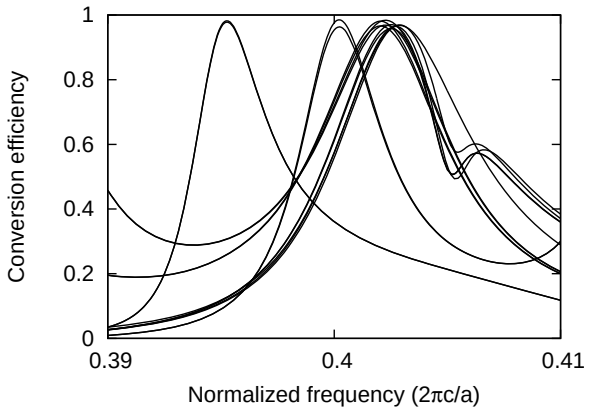


Fig. 8. Final candidate spectra obtained from the combinatorial search over $2^{20}$ possibilities at frequencies near $0.4 \times 2\pi c/a$. The vertical axis shows the conversion efficiency from mode A to mode D, and only spectra for structures with peak efficiency greater than 95% are shown.

spatial input and output modes by the number of frequencies, though we will not consider this further here. See Ref. [4] for a discussion of design complexity with multiple frequencies.

First, since the device is to be unitary, the device matrix is necessarily square (unitary transformations retain orthogonality, which requires the corresponding matrices are square, for example). For an $M \times M$ unitary matrix, to specify the first column of the matrix requires $2M-1$ real numbers (the "$-1$" arises because the sum of the modulus squared elements must equal 1, thus reducing the real degrees of freedom by 1 in the choice of these numbers). In general, for the second column of a unitary matrix, it must be orthogonal to the first column, which means both the real and imaginary parts of the inner product of these two columns must be zero, thereby reducing the number of degrees of freedom by 2, so that second column can only have $2M-3$ real degrees of freedom to specify it. Additionally, because the matrix here is to be symmetric, the top element of this column must be the same as the second row element of the first column, reducing the degrees of freedom by a further 2, leaving $2M-5$. For each successive column, if required, we reduce the degrees of freedom by a further 4. We only need to continue until we have specified half the columns (i.e., $M/2$); the other columns are then all known as a result of the matrix symmetry and the orthogonality of the columns. The total number of degrees of freedom (real numbers) to specify this unitary symmetric matrix is therefore

$$(2M-1)+(2M-5)+\cdots+\left[2M-4\left(\frac{M}{2}-1\right)-1\right]=\frac{M}{2}(M+1) \tag{2}$$

Since we do not care about the phase of the outputs relative to the inputs, we have one less real constraint for each of the $M/2$ columns we can specify, so the final complexity number for an arbitrary unitary symmetric operator with floating output phases is

$$N_D = M^2/2 \tag{3}$$

For our present devices, with $M=4$, we therefore have $N_D = 8$. That is, with 8 real degrees of freedom in our design, we would have enough variables in principle to design any such device with 4 input and output modes, including, therefore, the specific ones we have chosen to design. Note in our designs we have used 20 binary numbers in the simplest designs (namely,

#178467 - $15.00 USD Received 22 Oct 2012; revised 19 Nov 2012; accepted 23 Nov 2012; published 6 Dec 2012

the presence or absence of each of 20 rods). How we should relate the number of real numbers, $N_D$, required to the number of binary numbers used is not quantitatively clear, but we note we have used only a moderately larger number of binary variables here than $N_D$. This observation is similar to the behavior of the 3-mode-to-3-mode converter of [16], as considered in [4]. In our designs here, we have also adjusted the rod radius (a real number) in our final designs, though we note that this adjustment, though useful in some designs, did not make a large qualitative difference to the device performance.

## 5. Conclusion

We have demonstrated an extremely compact photonic crystal waveguide mode converter with a footprint of only 4 wavelengths in length. The device was designed by a process of global combinatorial search over the design space followed by a gradient-based optimization using a highly efficient tailored numerical method.

Additionally, we have presented a compact optical diode design with a length of only 2 wavelengths. It was discovered by a similar combinatorial search, and the subsequent gradient descent optimization not only increased the peak efficiency of the device, but also doubled its operating bandwidth. The number of degrees of freedom used in our designs compares well with estimated numbers required for such designs based on a complexity analysis. Our work highlights the substantial opportunities in the use of aperiodic structures for the control of optical modes.

## Acknowledgments

This work is supported in part by the United States Air Force Office of Scientific Research (US-AFOSR) grant FA9550-09-1-0704, and the National Science Foundation (NSF) grant DMS-0968809.

#178467 - $15.00 USD Received 22 Oct 2012; revised 19 Nov 2012; accepted 23 Nov 2012; published 6 Dec 2012